SCIENCE CHINA
Technological Sciences

November 2010 Vol.53 No.11: 3027–3032
doi: 10.1007/s11431-010-4116-z

A mechanism for enhanced photocatalytic activity of nano-size silver particle modified titanium dioxide thin films

MENG FanMing[1,2,3*], LU Fei[1,3], SUN ZhaoQi[1,3] & LÜ JianGuo[1,2,4]

[1] *School of Physics and Materials Science, Anhui University, Hefei 230039, China;*
[2] *Key Laboratory of Materials Modification by Laser, Ion and Electron Beams (Dalian University of Technology), Ministry of Education, Dalian 116024, China;*
[3] *Anhui Key Laboratory of Information Materials and Devices, Anhui University, Hefei 230039, China;*
[4] *Department of Physics and Electronic Engineering, Hefei Normal University, Hefei 230061, China*

Received June 8, 2010; accepted August 3, 2010

Ag-TiO_2 nanostructured thin films with silver volume fraction of 0–20% were deposited on silicon and quartz substrates by RF magnetron sputtering and annealed in ambient air at 950°C for 1 h. The phase structure and surface topography of the films were characterized by X-ray diffractometer and transmission electron microscope. Photocatalytic activity of the films was evaluated by light induced degradation of methyl orange ($C_{14}H_{14}N_3NaO_3S$) solution using a high pressure mercury lamp as lamp-house. The relation of photocatalytic activity and silver content was studied in detail. It was found that silver content influences phase structure of TiO_2 thin films, and silver in the films is metallic Ag (Ag^0). With increasing silver content from 0 to 20 vol%, photocatalytic activity of the films increases first and then decreases. A suitable amount (2.5–5 vol%) silver addition can significantly enhance the photocatalytic activity of TiO_2 films. The enhanced photocatalytic activity was mainly attributed to the extension of visible light absorption region of the films, the presence of anatase phase, the increase of oxygen anion radicals O_2^- and reactive center of surface Ti^{3+}, and the better separation between electrons and holes on the films surface.

silver, nanoparticle, TiO_2 thin film, photocatalytic activity, RF magnetron sputtering, methyl orange

Citation: Meng F M, Lu F, Sun Z Q, et al. A mechanism for enhanced photocatalytic activity of nano-size silver particle modified titanium dioxide thin films. Sci China Tech Sci, 2010, 53: 3027–3032, doi: 10.1007/s11431-010-4116-z

1 Introduction

In 1972, Fujishima and Honda [1] discovered the photocatalytic splitting of water on TiO_2 electrodes. This event marked the beginning of a new era in heterogeneous photocatalysis [2]. Recently, heterogeneous photocatalysis has attracted growing attention in which TiO_2 thin films is used as an advanced water treatment and water purification process. However, for practical application, the photocatalytic activity of the TiO_2 thin films needs a further improvement. As a result, much attention has been paid to the material doped with noble metals, such as Pt [3], Au [4], and Ag [5]. Among these metals, silver is widely used due to its efficient plasmon resonance in the visible region [6] and good antibacterial activity [7].

In this work, Ag-TiO_2 nanostructured thin films were deposited on silicon and quartz substrates by RF magnetron sputtering and annealed at 950°C for 1 h. The main purpose is to investigate the influence of silver content on phase structure, surface topography, and photocatalytic activity of the films.

---

*Corresponding author (email: mrmeng@ahu.edu.cn)

2 Experimental procedure

Ag-TiO_2 nanostructured thin films with various silver content were prepared by a high vacuum multifunctional magnetron sputtering equipment (JGP560I) using Ag-TiO_2 ceramic targets (ϕ=60 mm) on silicon (10 mm×10 mm) and quartz (25.1 mm×15.4 mm) substrates at room temperature. The targets were made by sticking Ag strips (99.99% purity) onto TiO_2 target (99.99% purity). Volume fraction of silver in the resulting films can be calculated [8] from eq. (1):

$$q_M = \frac{x m_M \rho_D S_{MD}}{x m_M \rho_D S_{MD} + m_D \rho_M}, \tag{1}$$

where, q_M is the volume fraction of silver in the resulting films, m_M and m_D is the molar mass of silver and TiO_2, ρ_M and ρ_D is the density of silver and TiO_2, $S_{MD}=v_M/v_D$ (v_M and v_D is sputtering rate of silver and TiO_2), and the value of S_{MD} is around 40.2 obtained by experimental measurements, $x=A_M/A_D$ (A_M and A_D is bare area of silver and TiO_2). Prior to deposition, the substrates were ultrasonically cleaned with acetone, absolute ethyl alcohol, and deionized water for 10 min, respectively. When the sputtering chamber was evacuated to a base pressure of 8×10^{-4} Pa, argon gas (99.99% purity) was introduced. Before the films were deposited, Ag-TiO_2 ceramic target was pre-sputtered by argon ion for 3 min to weed out the surface adsorption. During sputtering, argon gas flow rate was kept at 30 sccm, the chamber pressure was maintained at 0.8 Pa, the sputtering power was 60 W, and the distance between the substrate and the target was 60 mm. In order to obtain the same film thickness, sputtering time was 27, 25.3, 24, 22, and 18 min corresponding to silver content of 0, 2.5, 5, 10, and 20 vol%, respectively, due to their different sputtering rates. After deposition the films were annealed in ambient air at 950°C for 1 h.

The thickness of the films corresponding to silver content of 0, 2.5, 5, 10, and 20 vol%, measured by a surface profiler meter (Ambios XP-1), is 112, 116, 122, 109, and 112 nm, respectively. The crystallization behavior of the films was analyzed by an X-ray diffractometer (MAC M18XHF) using Cu Kα radiation. Surface morphological features were observed by a transmission electron microscope (JEM-2100).

Photocatalytic activity of the films was characterized by degradation of methyl orange ($C_{14}H_{14}N_3NaO_3S$). The experiment was performed in a 30 mL glass container. Lamp-house is a 36 W high pressure mercury lamp, which emits visible light of 404.7, 435.8, 546.1, and 577.0–579.0 nm, and ultraviolet light of 365 nm. Two samples of quartz substrate were horizontally placed at the bottom of the testing cell containing 10 mL 5 ppm methyl orange solution. The distance between the sample and the high pressure mercury lamp was 3.1 cm. The transmittance of the methyl orange solution was measured at intervals of 20 min and the total irradiation time was 3 h. The degradation rate of methyl orange could be obtained by

$$\eta = (C_0 - C_t)/C_0 \times 100\%, \tag{2}$$

where η is degradation rate of methyl orange after t min reaction, C_t is the concentration of methyl orange after t min reaction and C_0 is initial concentration.

3 Results and discussion

Figure 1 shows XRD patterns of 0, 2.5, 5, 10, and 20 vol% Ag modified TiO_2 thin films annealed at 950°C for 1 h. It can be seen that, for all the samples, there are diffraction angles of 27.70, 28.65, 38.37, and 39.33°, which correspond to the rutile (1 1 0), silicon (1 1 1), silver (1 1 1), and rutile (2 0 0), respectively. However, for 5 vol% Ag modified TiO_2 thin film, there are also diffraction angles of 25.80, and 31.04°, which correspond to anatase (1 0 1) and brookite (2 1 1); when silver content increases to 20 vol%, there is an additional diffraction angle of 44.57°, which corresponds to silver (2 0 0). Compared with other samples, 5 vol% Ag modified TiO_2 thin film shows more intense XRD diffraction peaks. In addition, the film exhibits an unexpected high degree of crystallization orientation along the anatase (1 0 1) planes. All these analyses suggest that silver content influences phase structure of TiO_2 thin films, and the addition of silver to the films is metallic Ag (Ag^0). It must be pointed out that silicon in Ag-TiO_2 thin films may form single crystal silicon substrate because of pervasion between substrate and the films when annealed at 950°C for 1 h.

Figure 2 shows TEM images of 0, 2.5, 5, 10, and 20 vol% Ag modified TiO_2 thin films as deposited. The distribution of silver particle in the films is uneven. With increasing silver content, the size and quantity of silver particles increase.

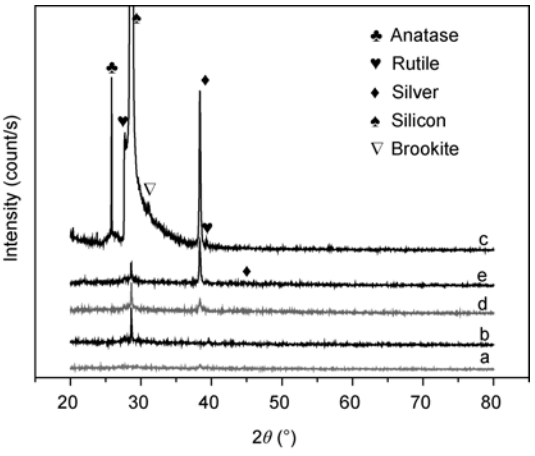

Figure 1 XRD patterns of (a) 0, (b) 2.5, (c) 5, (d) 10, and (e) 20 vol% Ag modified TiO_2 thin films annealed at 950°C for 1 h.

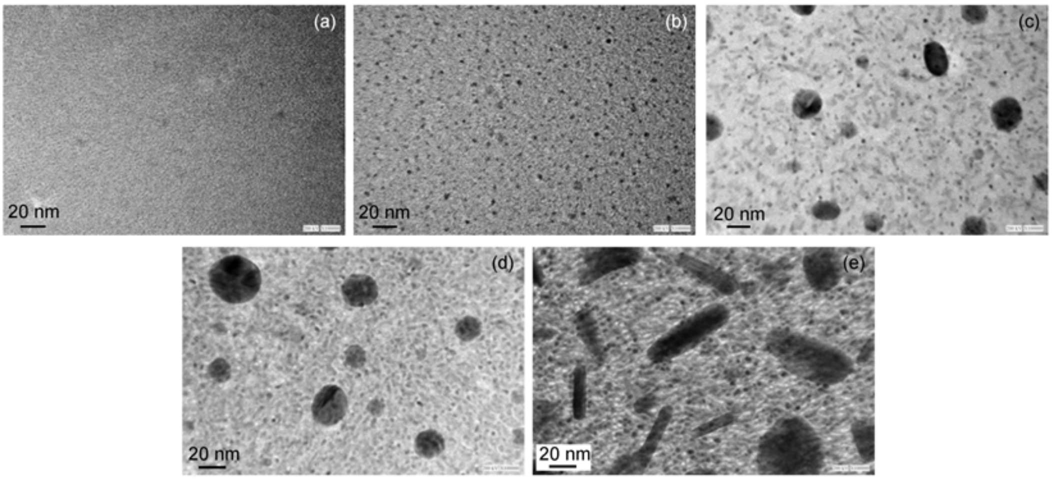

Figure 2 TEM images of (a) 0, (b) 2.5, (c) 5, (d) 10, and (e) 20 vol% Ag modified TiO_2 thin films as deposited.

In a previous study [9], we found that absorption spectra of methyl orange solution with various concentrations show two characteristic peaks at 270 and 464 nm, respectively, and absorbance of methyl orange solution at 464 nm is directly proportional to concentration. Therefore, in our study, the absorbance of peak at 464 nm is used to evaluate the absorption of methyl orange solution with various concentrations.

Figure 3 shows first-order kinetics of photocatalytic degradation of methyl orange as a function of irradiation time over 0, 2.5, 5, 10, and 20 vol% Ag modified TiO_2 thin films as deposited, where A_t is absorbance of methyl orange after t min reaction and A_0 is initial absorbance at 464 nm. From Figure 3, we can see that $\ln(A_0/A_t)$ is directly proportional to irradiation time. From the above analysis, absorbance of methyl orange solution is directly proportional to concentration. So, we can conclude that the photocatalytic degradation is first-order reaction and its kinetics can be expressed as follows:

$$\ln(C_0/C_t)=kt, \tag{3}$$

where C_t is the concentration of methyl orange after t min reaction, C_0 is the initial concentration, and k is apparent reaction rate constant. The photocatalytic activity can be compared by k value. The k values obtained by linear fitted from Figure 3 are 0.00303, 0.00307, 0.00332, 0.0027, and 0.00245 for the 0, 2.5, 5, 10, and 20vol% Ag modified TiO_2 thin films, respectively, as shown in Table 1. Based on absorbance of methyl orange solution at 464 nm, the concentration of methyl orange solution after 180 min reaction can be calculated [9], further, degradation rate of methyl orange can be obtained from eq. (1), as shown in Table 1. Degradation rate increases with increasing silver up to 5 vol% Ag and then decreases to values significantly smaller than that of pure TiO_2 thin films. With a suitable amount (2.5–5 vol% Ag), the silver addition increases the photocatalytic activity of the films. Among these films, 5 vol% Ag modified TiO_2 thin film exhibits the highest photocatalytic activity.

According to the principles of TiO_2 photocatalysis [10, 11], electron-hole pairs are generated when TiO_2 is irradiated with UV light. Separated electrons and holes diffuse to the surface of TiO_2 and then react with water, hydroxyl group and molecular oxygen adsorbed on TiO_2 producing reactive radicals, such as O_2^-, H_2O_2, and OH. These reactive radicals further react with organic and inorganic compounds adsorbed on TiO_2 and oxidize or reduce them. The reactions are summarized below [12, 13].

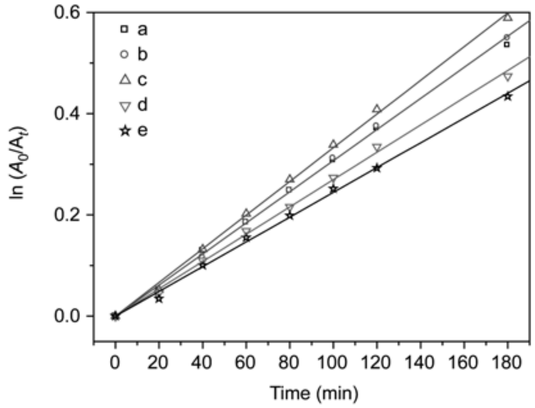

Figure 3 First-order kinetics of photocatalytic degradation of methyl orange as a function of irradiation time over (a) 0, (b) 2.5, (c) 5, (d) 10, and (e) 20 vol% Ag modified TiO_2 thin films annealed at 950°C for 1 h.

Table 1 Parameters of photocatalytic degradation of methyl orange over 0, 2.5, 5, 10, and 20 vol% Ag modified TiO_2 thin films annealed at 950°C for 1 h

Ag content (vol%)	0	2.5	5	10	20
Apparent reaction rate constant k (min^{-1})	0.00303	0.00307	0.00332	0.0027	0.00245
Degradation rate η (%)	46.07	46.93	49.23	42.32	39.73

$$TiO_2 \xrightarrow{hv} e^- + h^+ \tag{4}$$

$$e^- + O^2 \rightarrow O_2^- \tag{5}$$

$$h^+ + H_2O \rightarrow H^+ + OH \tag{6}$$

$$O_2^- + e^- + 2H^+ \rightarrow H_2O_2 \tag{7}$$

$$H_2O_2 \rightarrow 2OH \tag{8}$$

$$OH + \text{organic compounds} \rightarrow \text{products} \tag{9}$$

Generally speaking, the photocatalytic activity of the TiO_2 films is mainly dependent on three factors [14]: (1) the electron-hole pairs generation capacity; (2) separation efficiency of the photogenerated electron-hole pairs; and (3) charge transfer efficiency of electrons and holes to compounds absorbed on TiO_2.

First, the yield of the photogenerated electron-hole pairs depends upon the intensity of incident photons with energy exceeding or equaling to the Ag-TiO_2 thin films energy gap [14]. In a previous study [15], we found that the energy gap are 3.02, 3.00, 2.81, 2.87, and 2.92 eV, for 0, 2.5, 5, 10, and 20 vol% Ag modified TiO_2 thin films, respectively. It has also been calculated that threshold absorption wavelengths are 411.6, 414.4, 442.4, 433.1, and 425.7 nm, for 0, 2.5, 5, 10, and 20 vol% Ag modified TiO_2 thin films, respectively. It can be seen that the threshold absorption wavelength increases with increasing silver content up to 5 vol% Ag and then decreases. Since the high pressure mercury lamp emits visible light of 404.7, 435.8, 546.1, and 577.0–579.0 nm, and ultraviolet light of 365 nm, we can conclude that all the films can absorb the ultraviolet light of 365 nm and visible light of 404.7 nm, but as an exception, 5 vol% Ag modified TiO_2 thin film can also absorb visible light of 435.8 nm, which makes the film exhibit the highest photocatalytic activity.

Second, the addition of noble metals to a photocatalytic semiconductor can change the photocatalytic process by changing the semiconductor surface properties [16]. The metal can enhance the yield of a particular product or the rate of the photocatalytic reaction, which was first observed by Sato et al. [17]. Figure 4 is an illustration of the electron capture properties at the Schottky barrier of the metal in contact with a semiconductor surface. The picture schematically illustrates the small area of the semiconductor surface that the metal actually covers, which has been confirmed by the TEM images as shown in Figure 2. After excitation the electron migrates to the metal where it becomes trapped and electron-hole recombination is suppressed. The holes diffuse freely to the semiconductor surface where oxidation of organic species can occur. When the two species come in contact the Fermi levels of the metal and semiconductor align causing electrons to flow to the metal from the semiconductor [16]. The decrease in electron density within the semiconductor leads to an increase in the hydroxyl group acidity [18]. This in turn affects the photocatalytic process on the semiconductor surface.

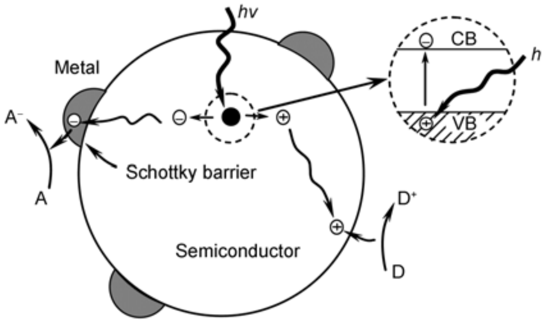

Figure 4 Schematic diagram showing metal modified semiconductor photocatalyst particle.

Third, small metal particles, of only several nanometers in diameter, deposited on semiconductor, have been reported to have enhanced photocatalytic efficiencies, as compared to larger sized deposits [19–21]. This has been attributed to the ability of the small metal particles to trap photoelectrons generated in the semiconductor. Large silver particles (Ag_n) on TiO_2 are considered to function as recombination sites, based on their ability to capture both photoelectrons and holes, as is consistent with literature values for the work function of bulk silver of –4.64 eV [22], positioning it within the TiO_2 band gap (top of valence band (VB) ≈−7.6 eV, bottom of conduction band (CB) ≈−4.4 eV) [22–24]. The electron affinity of a gas phase silver atom is reported to be −1.30 eV [22], the electron affinity of O_2 in the gas phase is –0.451 eV [25]. Based on these energy levels, as shown in Figure 5 for the Ag/TiO_2/O_2 system, which does not include consideration of Fermi level equilibration between contacting phases, it appears that bulk silver is energetically capable of accepting a photoelectron from the bottom of the TiO_2 conduction band, without substantial shift in Fermi level, but would not be capable of transferring this electron to a gas phase O_2 molecule to form the oxygen anion radicals, O_2^-. Transfer of a photoelectron from the bottom of the TiO_2 conduction band to a gas phase silver atom is energetically unlikely. This suggests a stabilization of the small Ag_n in contact with TiO_2, making possible the observed acceleration of O_2^- formation and the plausibility of the assignments shown in Figure 5 for Ag_n clusters occupying energetic positions below the vacuum level that range from −1.30 eV for $n = 1$, to that of the bulk silver work function of −4.64 eV, as n increases to large numbers yielding Ag_n sizes with properties approaching that of the bulk metal. For efficient electron transfer from the TiO_2 conduction band to Ag_n, a Ag_n electron accepting energy level must lie close to, or lower than −4.4 eV below the vacuum level. Since bulk silver does not efficiently lead to O_2^- formation, it would appear that the electron affinity of O_2 adsorbed on efficient Ag_n/TiO_2 photocatalysis is likely to be at higher energy than the bulk silver work function, –4.64 eV, and at lower energy than the bottom of the TiO_2 conduction band, –4.4 eV, as shown schematically in Figure 5. A sufficiently high number density of Ag_n particles on the TiO_2 surface could also lead to the increased recombination, as illustrated schematically in Figure 6.

A major role of surface deposition of small Ag_n on TiO_2 is attributed to acceleration of O_2^- formation [25], with the effect of decreasing recombination and increasing product yields initiated by h^+ or OH. The varied roles assigned to Ag_n, Ag_n as a function of size, are shown in reactions (10)–(12).

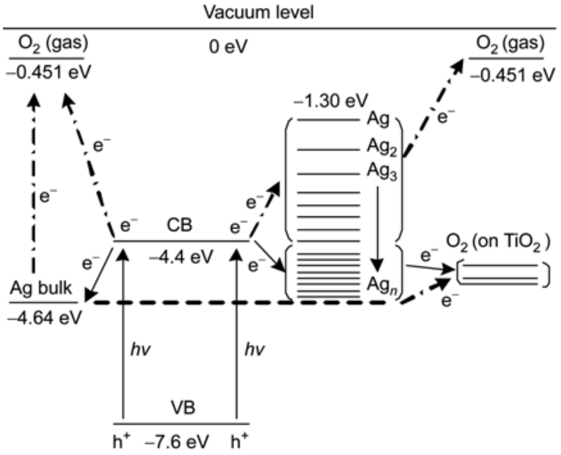

Figure 5 Schematic diagram showing the positions of the top of the TiO_2 valence band (VB), bottom of the TiO_2 conduction band (CB), the work function of bulk silver, a single atom of silver, the electron affinity of a gas phase O_2 molecule, and the required stabilization for oxygen anion radicals, O_2^-, formation when adsorbed to TiO_2, relative to the vacuum level = 0. Dotted arrow and solid arrow express impossible and possible, respectively.

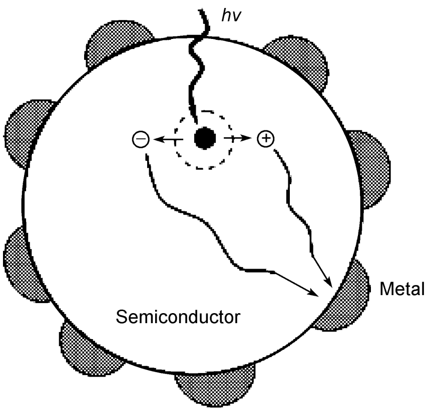

Figure 6 Schematic diagram showing high number density of silver particles can lead to increase in charge carrier recombination.

For small *n*,

$$e^- + Ag_n \rightarrow Ag_n^- \tag{10}$$

$$Ag_n^- + Ti^{4+} \rightarrow Ag_n + Ti^{3+}_{surface} \tag{11}$$

$$Ag_n^- + O_2 \rightarrow O_2^- + Ag_n \tag{12}$$

As the number and size of the Ag_n become sufficiently large, the silver deposits begin to function as recombination centers and the advantages of the metallic deposition are lost [25]. For large *n*, the energetic properties of the Ag_n may be approaching that of bulk Ag, reaction (13) competes with (12).

$$Ag_n^- + h^+ \rightarrow Ag_n \tag{13}$$

Based on geometric considerations, we proposed that a large number density of small epitaxial deposits on a semiconductor substrate is energetically capable of trapping photoelectrons, which would increase charge carrier recombination, whereas a smaller number of otherwise identical deposits may be effective in causing charge carrier separation [25, 26]. In addition, larger amount of silver would cover more TiO_2 surface and hinder the contact between TiO_2 and organic compounds, which would decrease the amount of the received photons [12].

Furthermore, it is noticeable that, compared with other samples, 5 vol% Ag modified TiO_2 thin film shows more intense XRD diffraction peaks and exhibits an unexpected high degree of crystallization orientation along the anatase (1 0 1) planes. It is well known that the anatase TiO_2 features the highest oxidizing power and the highest density of oxygen bridging sites [11] increasing the amount of anatase TiO_2 phase in the films is a prerequisite for increasing their photocatalytic activity [27]. Therefore, it is reasonable that 5 vol% Ag modified TiO_2 thin film exhibits the highest photocatalytic activity considering its especial phase structure.

4 Conclusion

Silver content influences phase structure of Ag-TiO_2 thin films. With increasing silver content, the size and quantity of silver particles increase to a certain extent, the energy gap of the films decreases first and then increases. And the photocatalytic degradation rate of methyl orange solution increases first and then decreases. Among these films, 5 vol% Ag modified TiO_2 thin film exhibits the highest photocatalytic activity. Silver addition can evidently improve visible light absorption of TiO_2 thin films and change the photocatalytic process by changing the films surface properties. A major role of surface deposition of small Ag_n on TiO_2 is attributed to acceleration of O_2^- formation, with the effect of decreasing recombination and increasing product yields initiated by h^+ or OH. As the number and size of the Ag_n become sufficiently large, the silver deposits begin to function as recombination centers and the advantages of the metallic deposition are gradually lost. The extension of visible light absorption region, the presence of anatase phase, the increase of O_2^- and Ti^{3+}, and the better separation between electrons and holes on the films surface are main causes of the enhanced photocatalytic activity for silver modified TiO_2 films.

This work was supported by the National Natural Science Foundation of China (Grant No. 50872001), the Scientific Research Foundation of Education Commission of Anhui Province of China (Grant Nos. KJ2009A006Z and KJ2007B132), the Doctor Scientific Research Starting Foundation of Anhui University of China, and the Foundation of Construction of Quality Project of Anhui University of China (Grant No. XJ200907).

1 Fujishima A, Honda K. Electrochemical photolysis of water at a semiconductor electrode. Nature, 1972, 238(1): 37–38

2 Yu Y, Yu J C, Chan C Y, et al. Enhancement of adsorption and photocatalytic activity of TiO_2 by using carbon nanotubes for the treatment of azo dye. Appl Catal B: Environ, 2005, 61(1-2): 1–11

3 Young C, Lim T M, Chiang K, et al. Photocatalytic oxidation of toluene and trichloroethylene in the gas-phase by metallised (Pt, Ag) titanium dioxide. Appl Catal B: Environ, 2008, 78(1-2): 1–10

4 Paramasivam I, Macak J M, Schmuki P. Photocatalytic activity of TiO_2 nanotube layers loaded with Ag and Au nanoparticles. Electrochem Commun, 2008, 10(1): 71–75

5 Kontapakdee K, Panpranot J, Praserthdam P. Effect of Ag addition on the properties of Pd–Ag/TiO_2 catalysts containing different TiO_2 crystalline phases. Catal Commun, 2007, 8(12): 2166–2170

6 Wang P, Huang B B, Qin X Y, et al. Ag@AgCl: A highly efficient and stable photocatalyst active under visible light. Angew Chem Int Ed, 2008, 47(41): 7931–7933

7 He X, Zhao X J, Liu B S. The synthesis and kinetic growth of anisotropic silver particles loaded on TiO_2 surface by photoelectrochemical reduction method. Appl Surf Sci, 2008, 254(6): 1705–1709

8 Xiao L, Cao C B, Song X P, et al. Microstructure and optical properties of nano Ag-ITO films. Sci China Tech Sci, 2010, 53(5): 1266–1270

9 Meng F M, Song X P, Sun Z Q. Photocatalytic activity of TiO_2 thin films deposited by RF magnetron sputtering. Vacuum, 2009, 83(9): 1147–1151

10 Choi W, Fermin A, Hoffmann M R. The role of metal ion dopants in quantum-sized TiO_2: correlation between photoreactivity and charge carrier recombination dynamics. J Phys Chem, 1994, 98(51): 13669–13679

11 Fujishima A, Rao T N, Tryk D A. Titanium dioxide photocatalysis. J Photochem Photobiol C: Photochem Rev, 2000, 1(1): 1–21

12 Liu S X, Qu Z P, Han X W, et al. A mechanism for enhanced photocatalytic activity of silver-loaded titanium dioxide. Catal Today, 2004, 93-95: 877–884

13 Xu M W, Bao S J, Zhang X G. Enhanced photocatalytic activity of magnetic TiO_2 photocatalyst by silver deposition. Mater Lett, 2005, 59(17): 2194–2198

14 He C, Yu Y, Hu X F, et al. Influence of silver doping on the photocatalytic activity of titania films. Appl Surf Sci, 2002, 200(1-4): 239–247

15 Meng F M, Lu F. Effect of silver content on energy gap and phase structure of silver-titania thin films prepared by radio frequency magnetron sputtering. J Chinese Ceram Soc, 2009, 37(12): 2130–2134

16 Linsebigler A L, Lu G Q, Yates J T. Photocatalysis on TiO_2 surfaces: principles, mechanisms, and selected results. Chem Rev, 1995, 95(3): 735–758

17 Sato S, White J M. Photodecomposition of water over Pt/TiO_2 catalysts. Chem Phys Lett, 1980, 72(1): 83–86

18 Jafiezic-Renault N, Pichat P, Foissy A, et al. Study of the effect of deposited platinum particles on the surface charge of titania aqueous suspensions by potentiometry, electrophoresis, and labeled-ion adsorption. J Phys Chem, 1986, 90(12): 2733–2738

19 Nakato Y, Tsubomura H. Structures and functions of thin metal layers on semiconductor electrodes. J Photochem, 1985, 29(1-2): 257–266

20 Ueda K, Nakato Y, Suzuki N, et al. Silicon electrodes coated with extremely small platinum islands for efficient solar energy conversion. J Electrochem Soc, 1989, 136(8): 2280–2285

21 Kobayashi H, Mizuno F, Nakato Y, et al. Hydrogen evolution at a platinum-modified indium phosphide photoelectrode: improvement of current-voltage characteristics by hydrogen chloride etching. J Phys Chem, 1991, 95(2): 819–824

22 Liu S X, Liu H. Photocatalysis and Photoelectrical Catalysis' Basic and Application (in Chinese). 1st ed. Beijing: Chemical Industry Press, 2006

23 Hoffmann M R, Martin S T, Choi W Y, et al. Environmental applications of semiconductor photocatalysis. Chem Rev, 1995, 95(1): 69–96

24 Herrmann J M. Heterogeneous photocatalysis: fundamentals and applications to the removal of various types of aqueous pollutants. Catal Today, 1999, 53(1): 115–129

25 Sadeghi M, Liu W, Zhang T G, et al. Role of photoinduced charge carrier separation distance in heterogeneous photocatalysis: oxidative degradation of CHOH vapor in contact with Pt/TiO and cofumed TiO-FeO. J Phys Chem, 1996, 100(50): 19466–19474

26 Gerisher H, Heller A. The role of oxygen in photooxidation of organic molecules on semiconductor particles. J Phys Chem, 1991, 95(13): 5261–5267

27 Mardare D, Luca D, Teodorescu C M, et al. On the hydrophilicity of nitrogen-doped TiO_2 thin films. Surf Sci, 2007, 601(18): 4515–4520